Supplementary

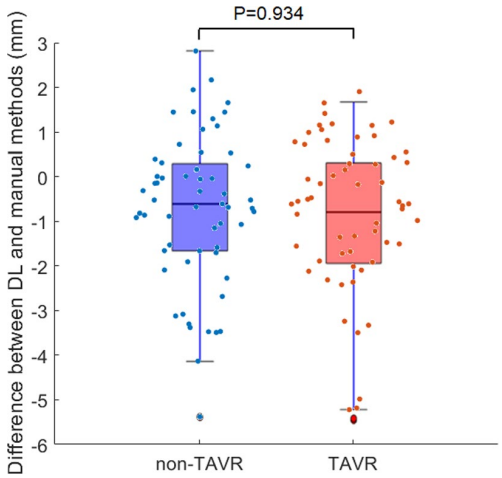

Figure S1 Comparison of the differences of annulus diameters between DL and manual methods between non-TAVR and TAVR groups. DL, deep learning; TAVR, transcatheter aortic valve replacement.

https://dx.doi.org/10.21037/qims-24-650

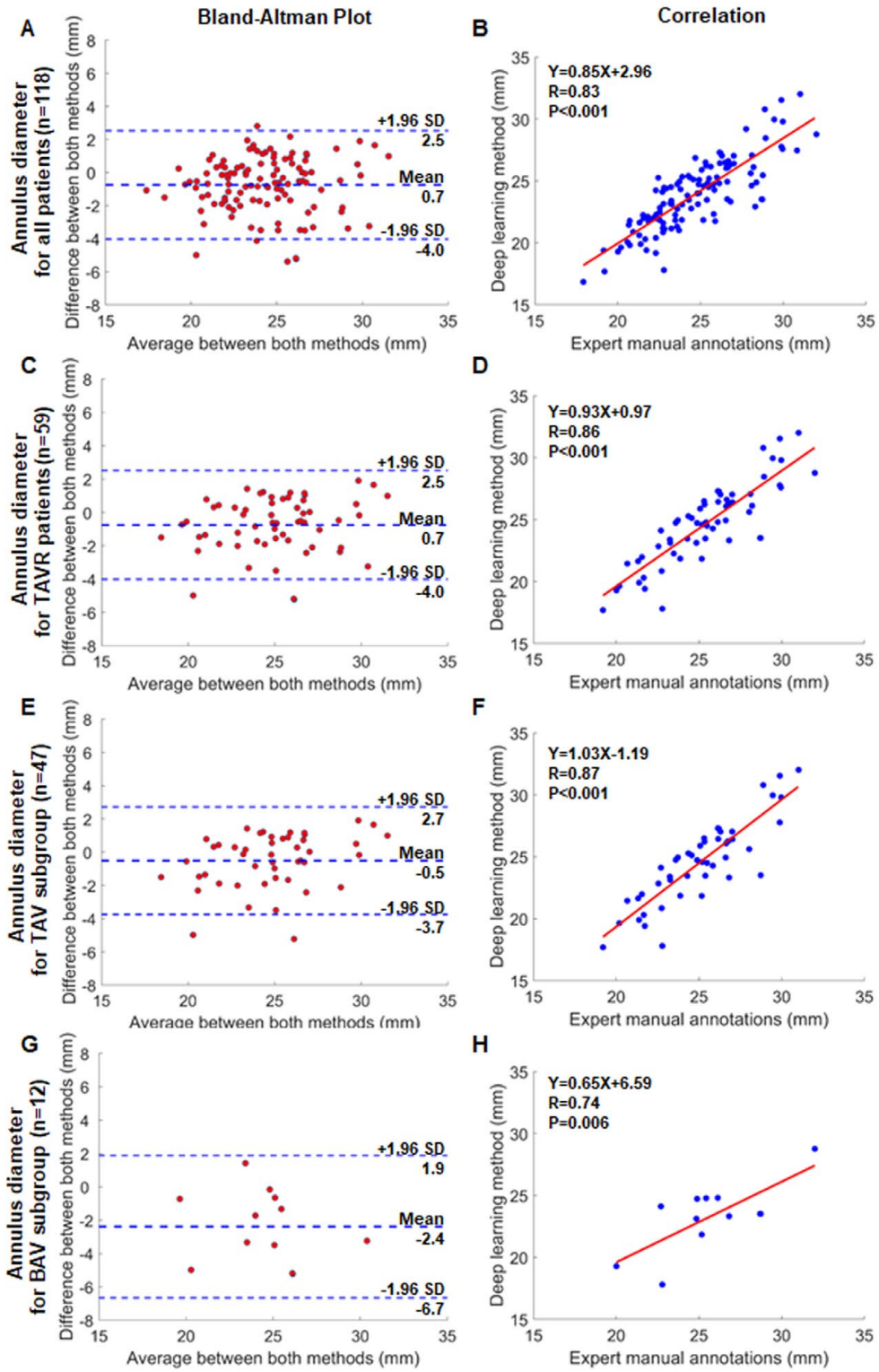

Figure S2 Bland-Altman plots and scatterplots of new deep learning analysis versus expert manual measurement for aortic annular mean diameter in the overall patient population (A,B), TAVR group (C,D), TAV (E,F) and BAV subgroups (G,H). TAVR, transcatheter aortic valve replacement; TAV, tricuspid aortic valve; BAV, bicuspid aortic valve.

https://dx.doi.org/10.21037/qims-24-650

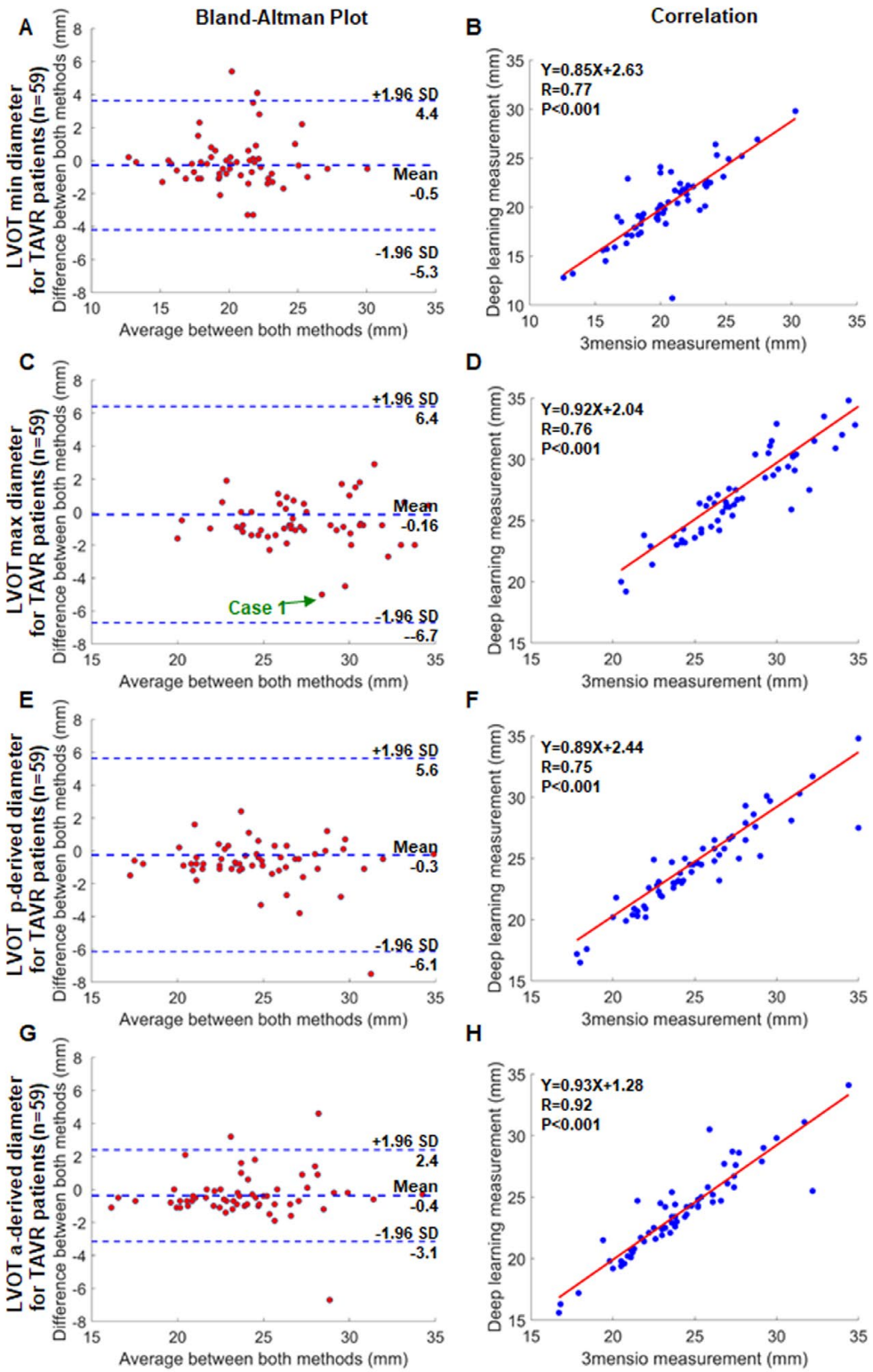

Figure S3 Bland-Altman plots and scatterplots of new deep learning analysis versus 3mensio software measurements for LVOT minimum (A,B), maximum (C,D), perimeter-derived (E,F) and area-derived (G,H) diameter in the TAVR patients. LVOT, left ventricular outflow tract; TAVR, transcatheter aortic valve replacement.

https://dx.doi.org/10.21037/qims-24-650

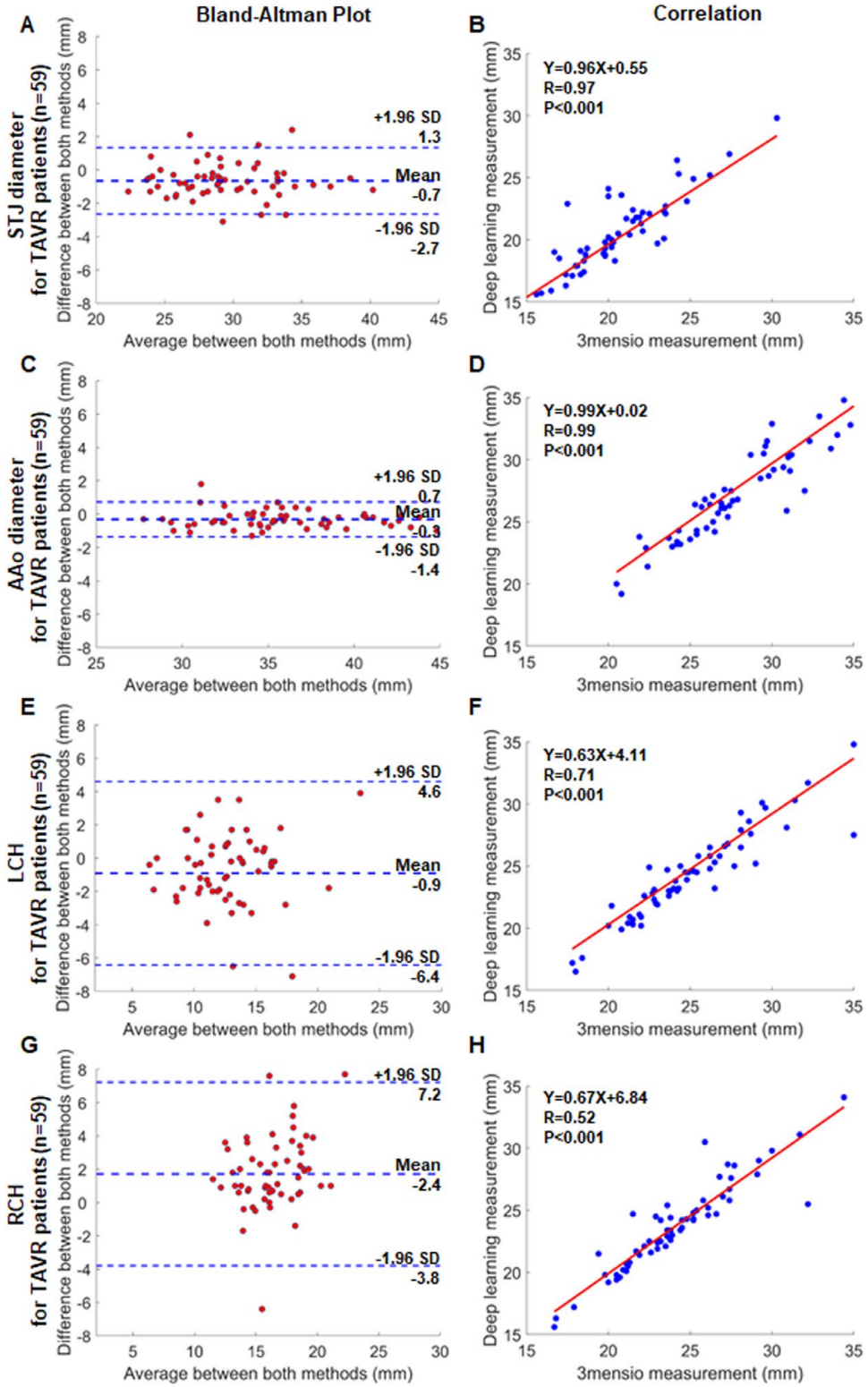

Figure S4 Bland-Altman plots and scatterplots of new deep learning analysis versus 3mensio software measurements for STJ (A,B) and AAo (C,D) diameter, and left (E,F) and right (G,H) coronary ostium heights in the TAVR patients. TAVR, transcatheter aortic valve replacement; STJ, sinotubular junction; AAo, ascending aorta; LCH, height of left coronary ostium; RCH, height of right coronary ostium.

https://dx.doi.org/10.21037/qims-24-650

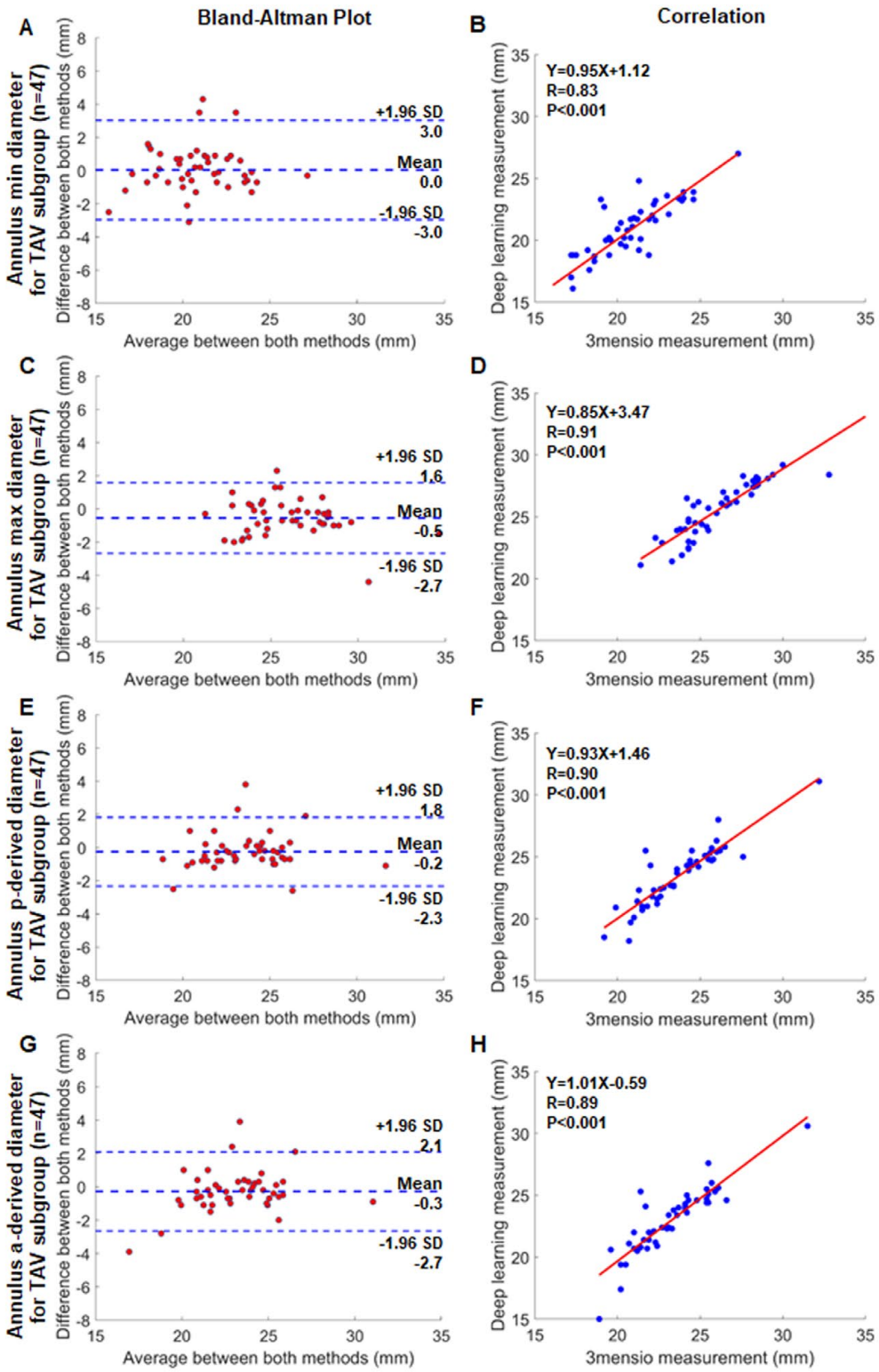

Figure S5 Bland-Altman plots and scatterplots of new deep learning analysis versus 3mensio software measurements for annulus minimum (A,B), maximum (C,D), perimeter-derived (E,F) and area-derived (G,H) diameter in the TAV subgroup. TAV, tricuspid aortic valve.

https://dx.doi.org/10.21037/qims-24-650

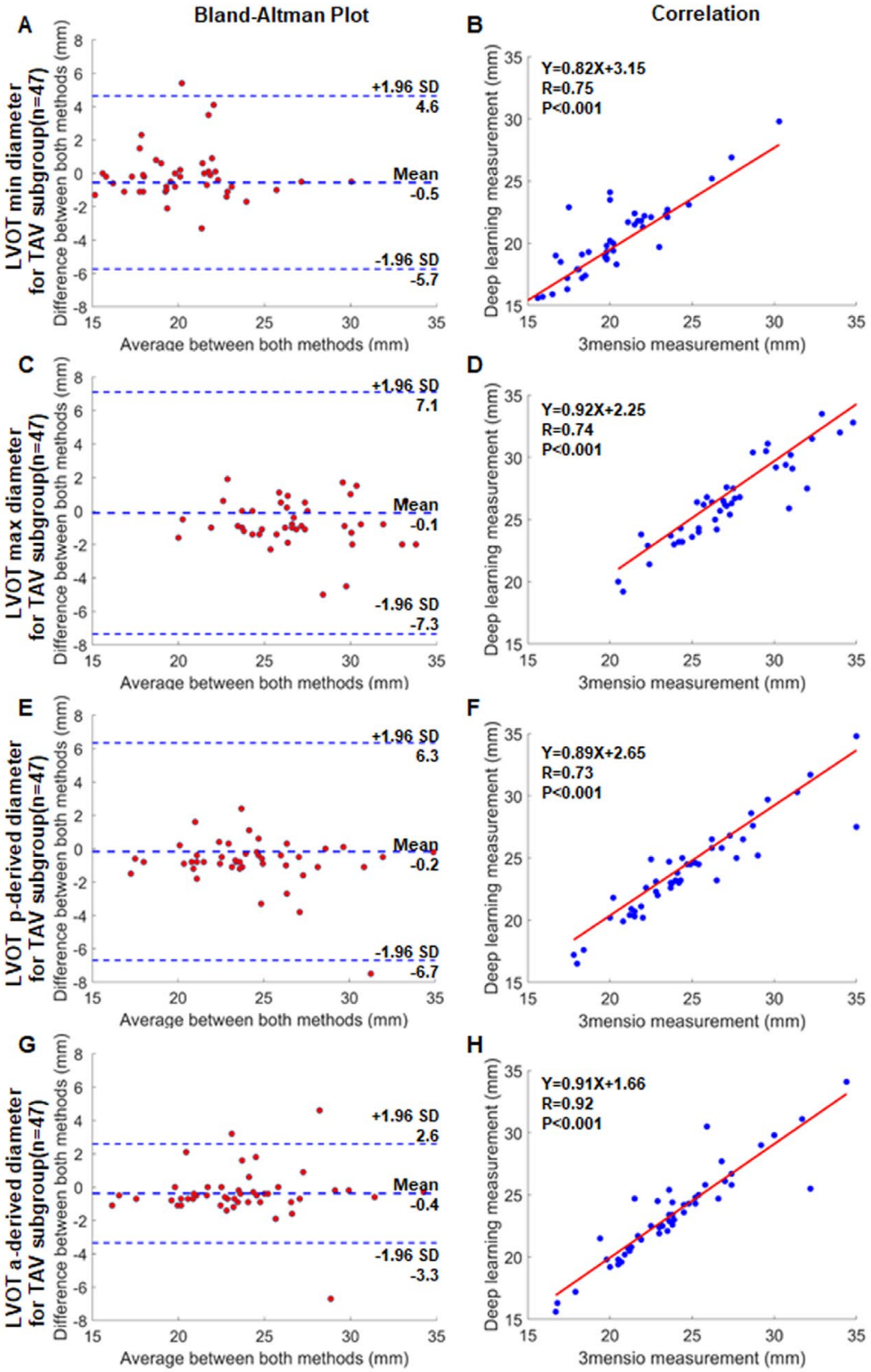

Figure S6 Bland-Altman plots and scatterplots of new deep learning analysis versus 3mensio software measurements for LVOT minimum (A,B), maximum (C,D), perimeter-derived (E,F) and area-derived (G,H) diameter in the TAV subgroup. TAV, tricuspid aortic valve; LVOT, left ventricular outflow tract.

https://dx.doi.org/10.21037/qims-24-650

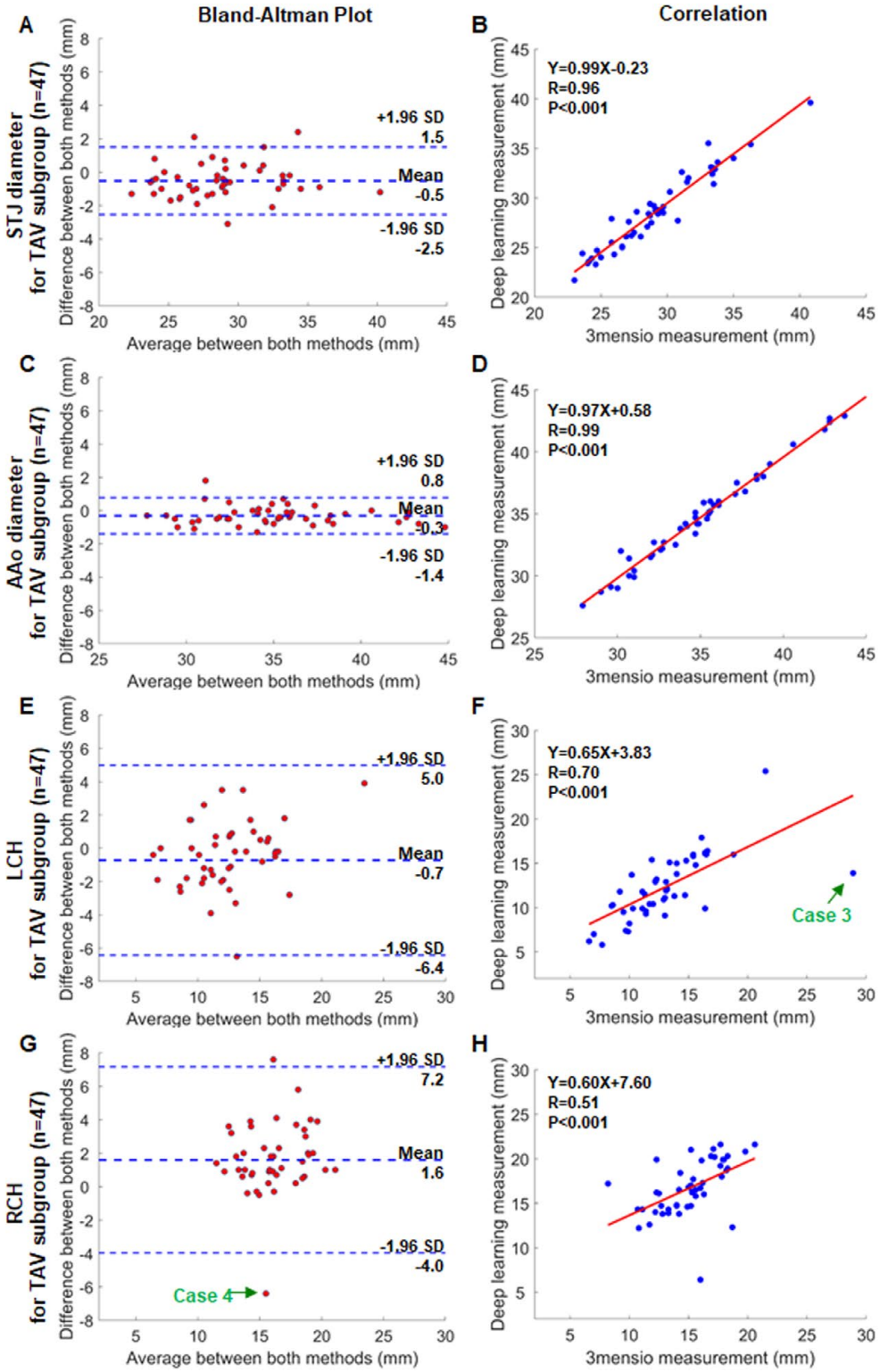

Figure S7 Bland-Altman plots and scatterplots of new deep learning analysis versus 3mensio software measurements for STJ (A,B) and AAo (C,D) diameter, and left (E,F) and right (G,H) coronary ostium heights in the TAV subgroup. TAV, tricuspid aortic valve; STJ, sinotubular junction; AAo, ascending aorta; LCH, height of left coronary ostium; RCH, height of right coronary ostium.

https://dx.doi.org/10.21037/qims-24-650

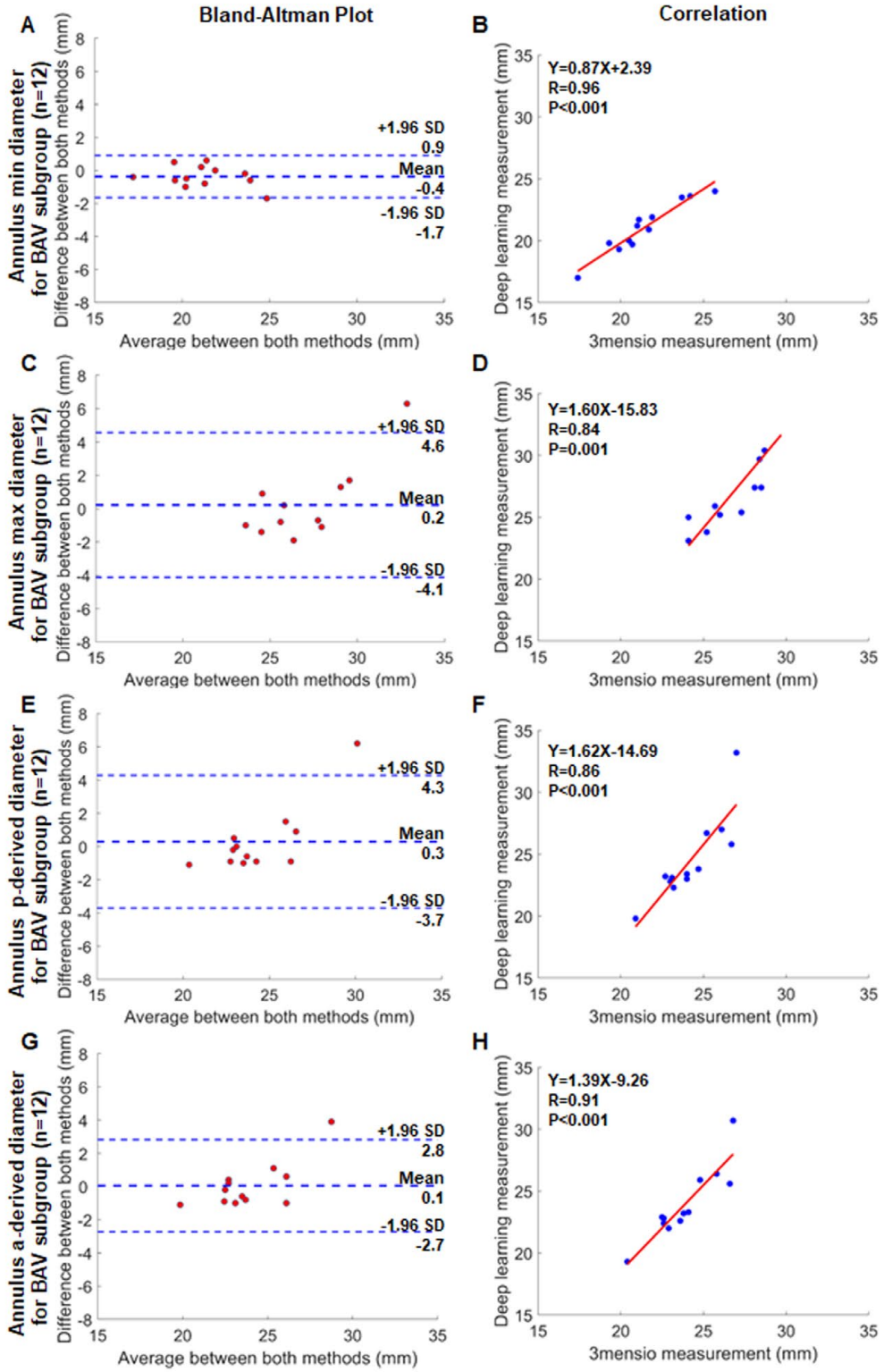

Figure S8 Bland-Altman plots and scatterplots of new deep learning analysis versus 3mensio software measurements for annulus minimum (A,B), maximum (C,D), perimeter-derived (E,F) and area-derived (G,H) diameter in the BAV subgroup. BAV, bicuspid aortic valve.

https://dx.doi.org/10.21037/qims-24-650

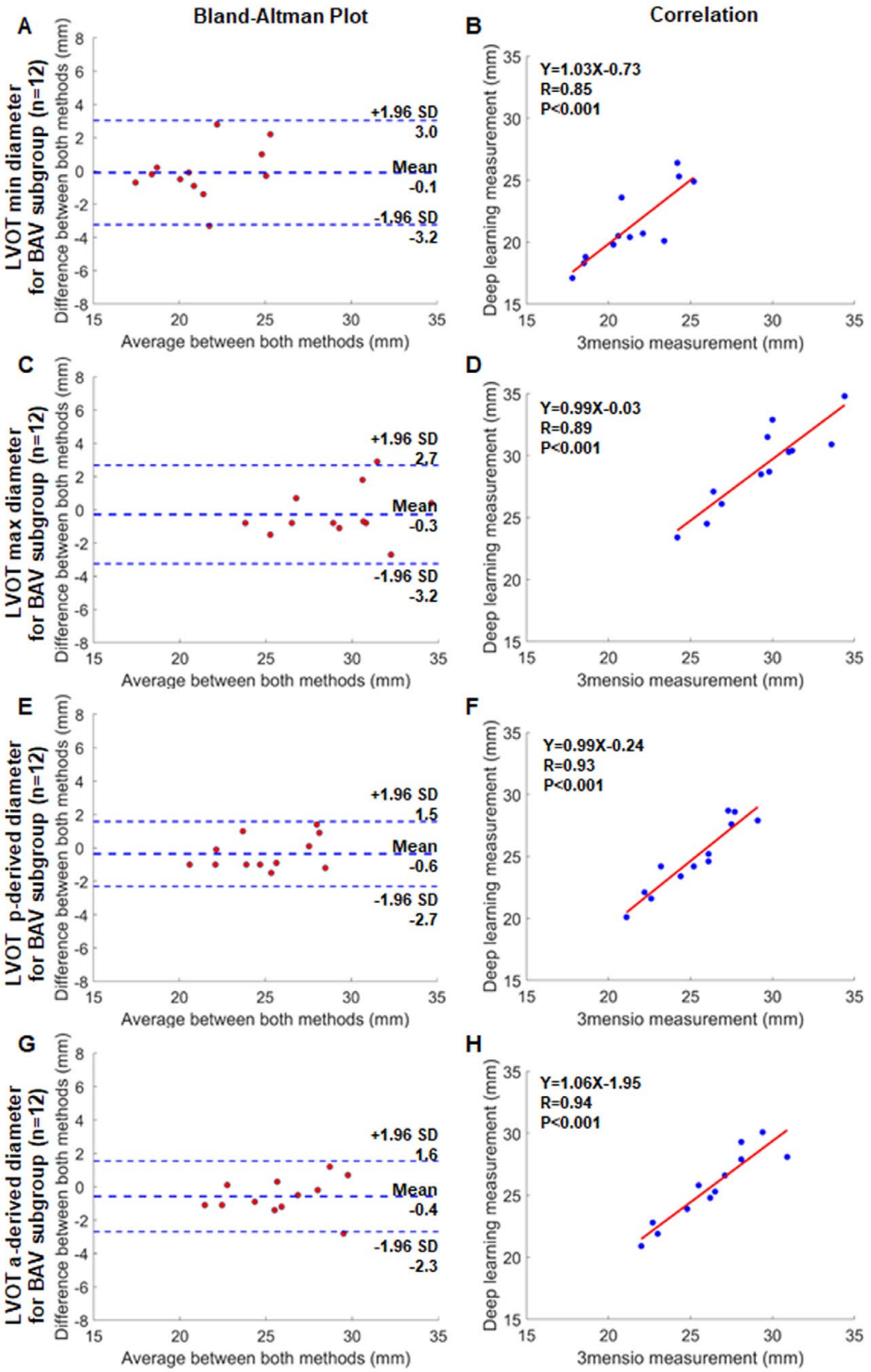

Figure S9 Bland-Altman plots and scatterplots of new deep learning analysis versus 3mensio software measurements for LVOT minimum (A,B), maximum (C,D), perimeter-derived (E,F) and area-derived (G,H) diameter in the BAV subgroup. BAV, bicuspid aortic valve; LVOT, left ventricular outflow tract.

https://dx.doi.org/10.21037/qims-24-650

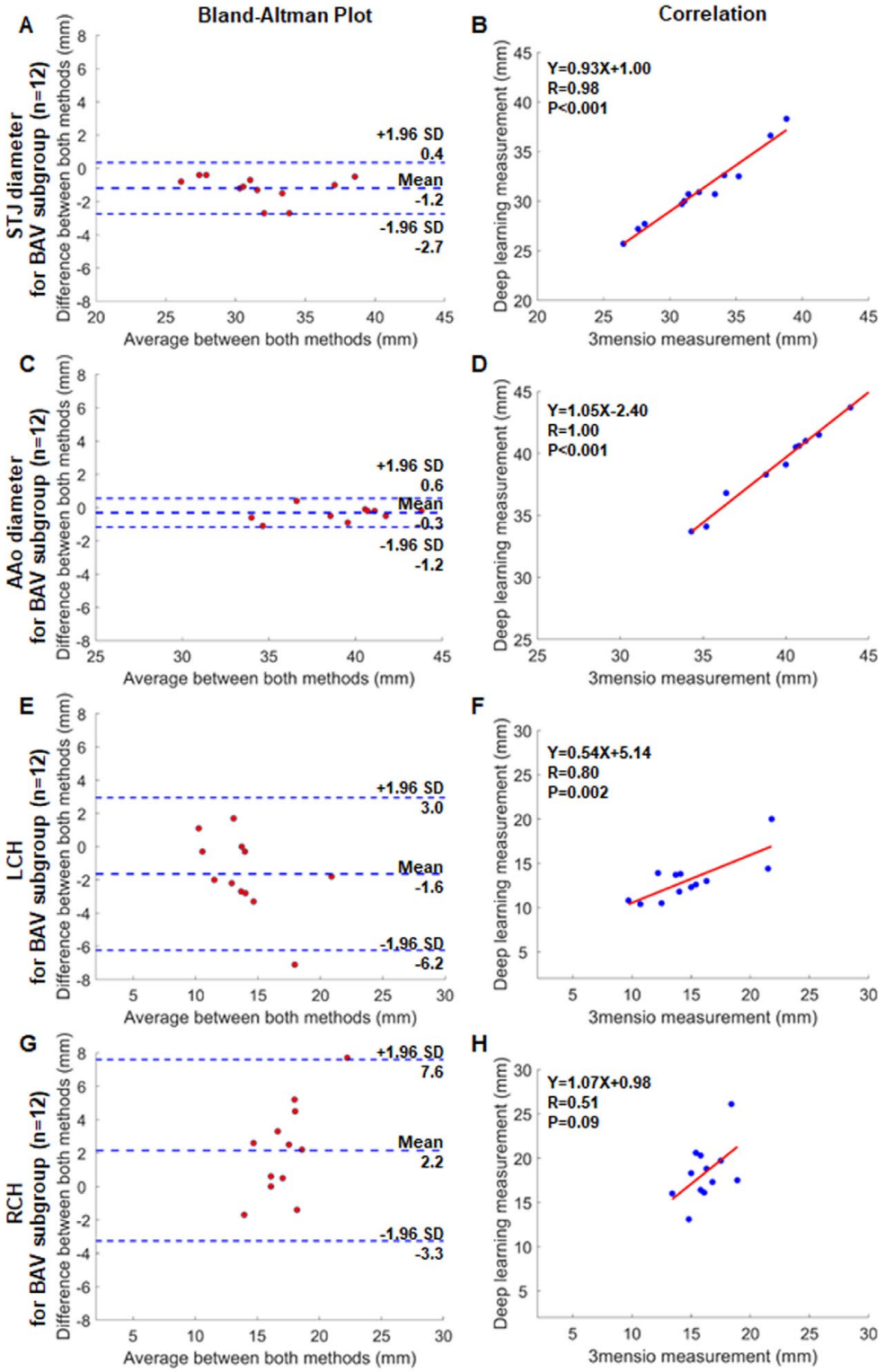

Figure S10 Bland-Altman plots and scatterplots of new deep learning analysis versus 3mensio software measurements for STJ (A,B) and AAo (C,D) diameter, and left (E,F) and right (G,H) coronary ostium heights in the BAV subgroup. BAV, bicuspid aortic valve; STJ, sinotubular junction; AAo, ascending aorta; LCH, height of left coronary ostium; RCH, height of right coronary ostium.

https://dx.doi.org/10.21037/qims-24-650

Video S1 Fully automated measurement of aortic root by the deep learning system in 2 minutes.

https://dx.doi.org/10.21037/qims-24-650